Cylindrical magnetron discharges. II. The formation of dc bias in rf-driven discharge sources

G. Y. Yeom and John A. Thornton[a)]
University of Illinois, Coordinated Science Laboratory, Urbana, Illinois 61801

Mark J. Kushner[b)]
University of Illinois, Gaseous Electronic Laboratory, 607 East Healey, Champaign, Illinois 61820

(Received 18 July 1988; accepted for publication 5 January 1989)

When a steady-state capacitive rf discharge is sustained between two electrodes whose surfaces in contact with the plasma have different areas, a negative dc self-bias usually develops on the smaller electrode. For ratios of electrode areas greater than about three, the self-bias is typically 80%–90% of the zero-to-peak potential of the applied rf voltage. However, in cylindrical-post magnetron discharges which are driven by rf power, the self-bias is often only 10%–20% of the zero-to-peak applied voltage. Since these discharges are of interest to both sputtering and plasma-assisted etching, we have investigated the formation of the dc self-bias as a function of applied magnetic field strength. We studied discharges using different diameter post electrodes at rf frequencies of 1.8 and 13.56 MHz. The self-bias voltages were indeed found to be considerably less than those observed in nonmagnetron discharges. Electrostatic probes were used to measure the interelectrode potential distribution. From these results we conclude that the reduced dc self-bias in rf driven cylindrical magnetron discharges can be explained in terms of the effect of the axial magnetic field on electron transport to the cylindrical-post electrode during that portion of the rf cycle when the post electrode is serving as an anode.

I. INTRODUCTION

In rf plasma discharge systems, such as those used for the deposition or etching of insulating materials, each electrode is bombarded by positive ions. As a result, one does not have a well-defined cathode. Thus an important aspect of rf sputtering technology is the ability to control the voltage drops within the plasma sheaths at the two electrodes. In doing so, one would like to insure that the target electrode is bombarded with ions of sufficient energy to produce the desired sputtering, while ion bombardment at the other electrode, on which substrates are often mounted, does not damage the growing film or introduce contamination into the system.[1]

Under certain operating conditions a dc self-bias develops in an rf discharge and assists in providing the desired voltage division. In particular, for the capacitively coupled discharges of primary interest for sputtering and plasma-assisted etching, there can be no net dc current flow. As a result the overall charge flow per cycle between the electrodes must sum to zero, and the total electron current per cycle to a given electrode must be equal to the total ion current per cycle.[2] When this requirement is coupled with the differences in mobility between the electrons and ions passing through the sheath at an electrode, an asymmetric voltage division will develop if there is a difference in the electrode areas in actual contact with the plasma. For electropositive plasmas the voltage division can be characterized as an induced negative dc self-bias of the smaller target electrode relative to the larger substrate electrode.[3]

A simple model for the dc bias in rf discharges has been proposed by Koenig and Maissel.[4] In this model a uniform plasma covers both electrodes with purely capacitive sheaths. For these conditions the ratio of the voltage drops within the two electrode sheaths are predicted to vary inversely with the fourth power of the electrode area ratio. Experimental data by Coburn and Kay[5] and Horwitz[6] suggest that the fourth power relationship is approximately valid for ratios near unity (< 1.6), but becomes less accurate for larger area ratios. A recent analysis by Savas[7] treats the plasma as a fluid with radial ion flow between concentric spherical electrodes. This work yields a dc bias versus area ratio relationship which is more complex than a power law because the sheath impedances are more resistive or more capacitive at different times in the rf cycle. The relationships obtained by Savas agree with the fourth power law at small area ratios (< 1.5), and also fairly reproduce the Coburn–Kay experimental data at larger area ratios. For example, a dc self-bias equal to about 90% of the zero-to-peak applied voltage is predicted by the fourth power law with an area ratio of about 2. The Savas model predicts this bias for an area ratio of about 5. The experimental data of Coburn and Kay obtained with an area ratio of 8 to 10. By capitalizing on the ability to change the energy of ions striking an electrode by selecting the appropriate area ratio, one may optimize sputtering and etching processes. Accordingly, the technique of using a "controlled area ratio of electrodes" (CARE) to induce an asymmetry in the electrode ion bombardment energies has become an important element of rf sputtering technology.[8]

[a)] Deceased.
[b)] Author to whom correspondence should be addressed.

 0021-8979/89/103825-08$02.40

Preliminary experiments have been performed to investigate the dc bias in cylindrical magnetron discharges.[9] In experiments conducted at 1.8 MHz with a device having a large area ratio, a dc self-bias of only about 10% of the zero-to-peak voltage was obtained with a magnetic field strength of 200 G.[10,11] As the magnetic field was decreased to zero, the dc bias increased to about 70% of the zero-to-peak voltage, as one would expect in nonmagnetron discharges. The absence of a significant dc self-bias in rf cylindrical-post magnetron discharges (13.56 MHz) has also been noted by Lin.[12]

This paper reports a systematic investigation of the formation of dc self-bias in cylindrical-post magnetron discharges of various diameters driven at rf frequencies of 1.8 and 13.56 MHz while using magnetic field strengths from 0 to 200 G. As expected, the dc self-bias levels were found to be a function of the magnetic field strength. To investigate the origin of the reduced self-bias, electrostatic probes were used to measure the interelectrode potential distribution in the plasmas. We conclude that the reduced dc self-bias in rf-driven cylindrical magnetrons can be explained by the effect of the magnetic field on the electron transport to the cylindrical-post electrode during that portion of the rf cycle when the post electrode is serving as an anode. The effect of the magnetic field on the current-voltage characteristics of rf-driven cylindrical-post magnetron discharges is discussed in a companion paper.[13]

II. EXPERIMENTAL APPARATUS

Details of the apparatus used in this investigation are discussed in Ref. 13. The chamber is constructed of type 304 stainless steel and configured to axially mount flange-type cylindrical-post magnetron electrodes of various diameters which are also made of stainless steel. The sizes of the cylindrical electrodes used for the present study are 12.7, 25.4, and 100 mm diam. Magnetic field coils are arranged at each end of the chamber in a magnetic back-strap configuration that provided a relatively uniform ($\pm$ 10%) magnetic field with strengths up to 200 G in the region occupied by the post electrodes while leaving the chamber walls accessible to plasma diagnostics instrumentation.[14] Screens (200 $\times$ 200 stainless-steel wire cloth) were placed over all of the chamber ports so that the grounded discharge chamber provided a relatively well-defined cylindrical-hollow counterelectrode when rf potential was applied to the central post electrode. The power supplies and data acquisition systems are the same as those discussed in Ref. 13.

Experiments were conducted during which the dc self-bias was measured as a function of magnetic field strength for fields ranging from 0 to 200 G, and at frequencies of 1.8 and 13.56 MHz. The rf frequencies were selected to investigate conditions characterized by primarily resistive and primarily capacitive sheath behavior.[7,15-17] The discharge current densities were in the range from 3 to 6 mA/cm^2. The working gas was Ar at a pressure of 0.4 Pa.

The radial variation in floating potential across the chamber at the cathode midplane was measured relative to ground potential using an electrostatic probe. The probe consists of a molybdenum disk tip 5 mm in diameter $\times$0.1 mm thickness, or a cylindrical tungsten tip 0.25–0.64 mm in diameter $\times$5 mm long. The probe was supported by a tubular quartz insulator having a shielded tip[16] to prevent shorting from conducting paths generated by sputtered stainless steel. The cylindrical probe was also used as a Langmuir probe to estimate the electron temperature so that the plasma potential could be estimated from the floating potential measurements. In order to provide an independent value of the plasma potential, the energy distributions of ions incident on the midplane of the chamber wall were measured using the retarding grid electrostatic analyzer shown in Fig. 1.

III. MEASUREMENTS OF dc BIAS AND PLASMA PARAMETERS

The variations in the dc bias voltage relative to the zero-to-peak applied voltage for the three post electrodes driven at 1.8 and 13.56 MHz are shown in Fig. 2. In all cases the rms discharge currents were adjusted to yield a nominal current density of about 3 mA/cm^2. It should be noted, however, that the actual power input to the plasma was found to be dependent on magnetic field strength because of the influence of the magnetic field on the phase relation between the current and voltage. Typical oscilloscope traces for the discharge current and voltage are shown in Figs. 3 and 4. At zero magnetic field the discharge current leads the applied voltage by 80°–88°. The average phase difference decreased with magnetic field strength so that at 200 G the phase differences were generally less than 60°. General trends are illustrated in Fig. 5. The phase shift decreased, as would be expected, with working gas pressure and tended to be less for

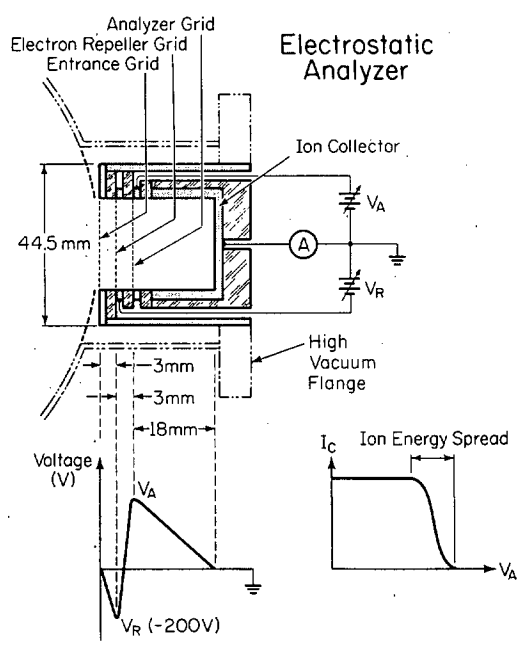

FIG. 1. Schematic diagram of the retarding grid electrostatic analyzer. The analyzer was mounted on the side wall of the experimental chamber. (See Ref. 13.)

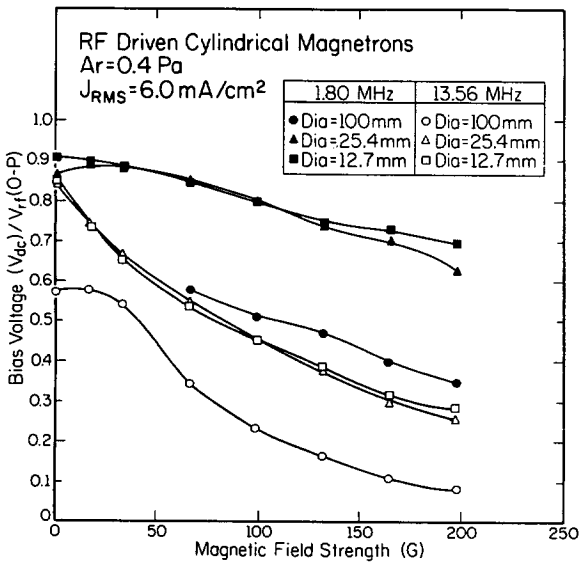

FIG. 2. Influence of the magnetic field strength on dc self-bias voltage relative to zero-to-peak voltage for cylindrical magnetron discharge sources driven at 1.8 and 13.56 MHz.

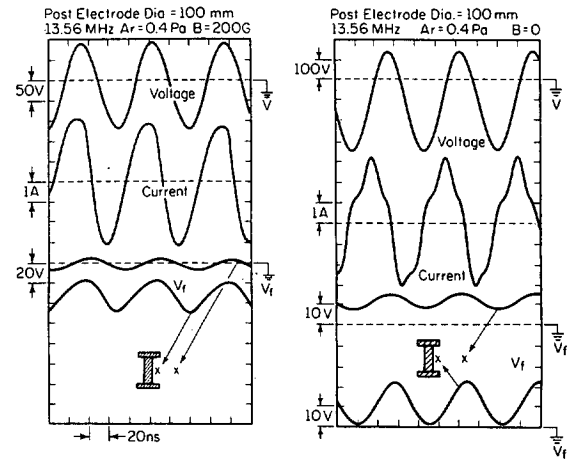

FIG. 4. Time dependence of the discharge voltage, discharge current, and floating potential for a discharge with a 100-mm-diam post electrode driven at 13.56 MHz. Left-hand side, $B = 200$ G; right-hand side, $B = 0$ G. The crosses show the location of the probe measurement.

1.8 MHz excitation and for the larger post electrode diameters. The reduction in phase angle with increasing magnetic field indicates that the sheaths are becoming more resistive (as opposed to capacitive). The ratio of the dc self-bias voltage to the zero- to-peak applied voltage shown in Fig. 2 was not constant for different current densities. As the current density is increased, the ratio tends to increase and particularly so at the high magnetic field strengths. However, for all the cases investigated, the ratio at different current densities had the same functional relationship on magnetic field strength as shown in Fig. 2.

The time dependencies of the floating potentials at a radial position within the end flanges of the cylindrical electrodes are shown in Figs. 3 and 4. The time dependence of the floating potential at 1.8 MHz with an applied magnetic field of 200 G is typically what one would expect with largely resistive sheaths at the discharge electrodes. Under these conditions the floating potential has the same time dependence as the plasma potential since both ions and electrons can cross the sheaths in times that are short compared to the rf period.[14] The floating potential at 1.8 MHz with no magnetic field, though, has a time dependence intermediate between capacitive and resistive. This may result from having thick sheaths (low plasma density), where the ions cannot cross the probe sheath in a single rf period.[15] The trends in floating potential as a function of magnetic field, and their implications on sheath behavior, are consistent with our measurements of phase angle. The time dependencies of floating potential at 13.56 MHz (Fig. 4) are suggestive of

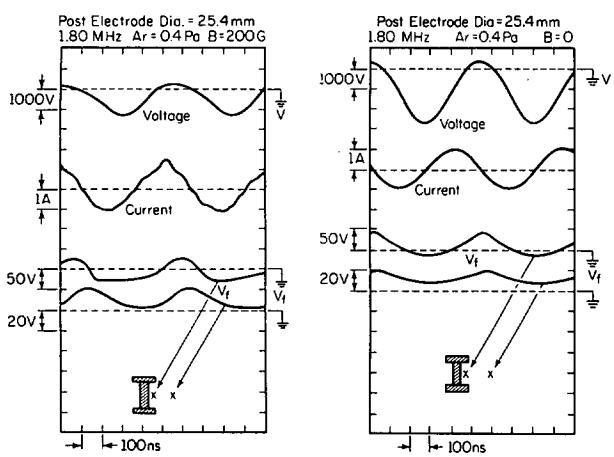

FIG. 3. Time dependence of the discharge voltage, discharge current, and floating potential for a discharge with a 25.4-mm-diam post electrode driven at 1.8 MHz. Left-hand side, $B = 200$ G; right-hand side $B = 0$ G transfer to the plasma. The crosses show the location of probe measurements. The data shows the effect of the magnetic field in decreasing the phase difference between the current and voltage and increasing the power transfer to the plasma.

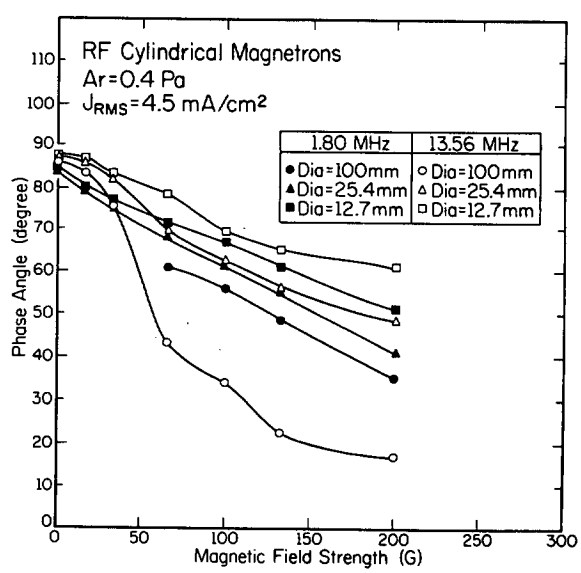

FIG. 5. Influence of the magnetic field strength on the average phase difference between the discharge current and voltage.

largely capacitive sheath behavior, as one would expect at the higher frequency.

In order to better understand the origin of the reduction in self-bias with increasing magnetic field, we measured the radial variation in the plasma potential. Due to difficulties in directly measuring the plasma potential in an rf plasma, the plasma potential was deduced from floating potential, electron temperature, and electrostatic ion energy analyzer measurements. The radial variations in positive and negative extremes of the floating potential at the cathode midplane are shown in Fig. 6 for the 12.7-mm-diam electrode driven at 1.8 MHz and 13.56 MHz. Data are shown for the zero magnetic field and 200-G cases. The plasma potential will exceed the floating potential by an amount, for a Maxwellian electron velocity distribution is given by

$$V_p - V_f = (kTe/2e)\ln(M_i/2.3m_e),$$

where kT_e is the electron temperature and M_i and m_e are the ion and electron masses.[1] Thus for a well-defined electron temperature in Ar, $V_p - V_f$ is about $5kT_e$. Operating the electrostatic probe as a Langmuir probe we obtained nearly linear time-averaged log-current versus bias voltage curves. These curves suggested that the average electron temperatures were approximately 12 eV for experimental conditions shown in Fig. 6. The electron temperature, though, was a function of radial position and was generally higher close to the post electrode where energetic secondary electrons are more likely to be found.

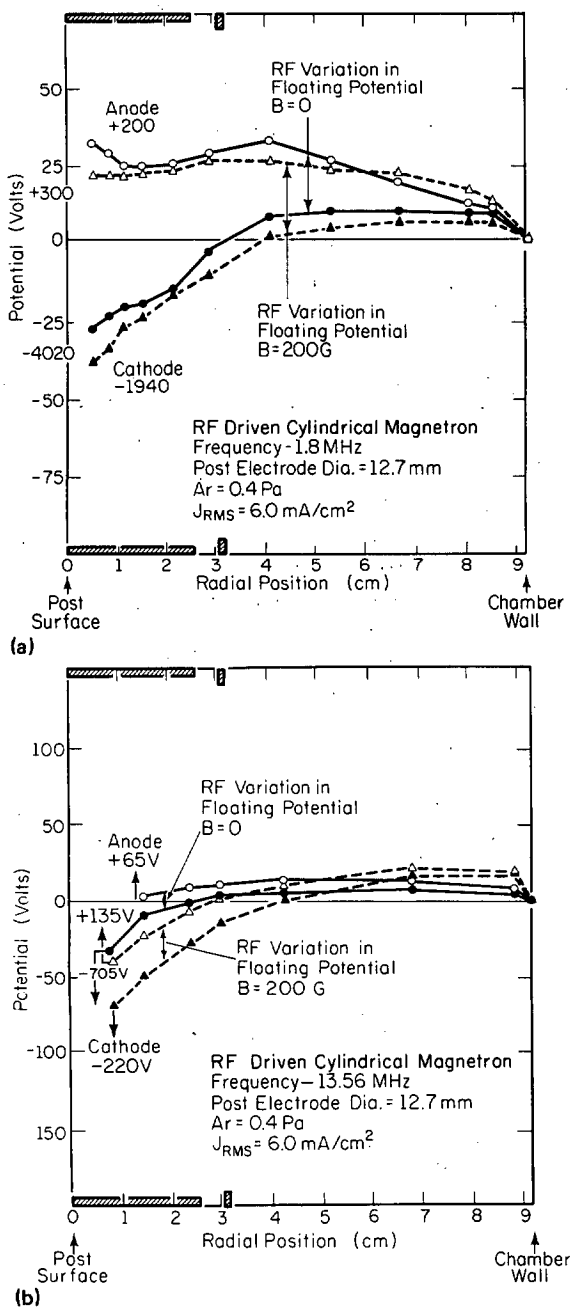

FIG. 6. Maximum positive and negative values of the floating potential vs radial position along the vertical midplane for a discharge using a 12.7-mm-diam post electrode driven at (a) 1.8 and (b) 13.56 MHz. The "anode" and "cathode" voltages are the peak positive and negative voltage excursions of the post electrode. All voltages are given relative to the grounded chamber. Data are given for magnetic fields of 0 and 200 G.

As a further check on our estimation of plasma potential, the electrostatic analyzer on the midplane of the grounded chamber wall was used to measure the energy distribution of the incident ions. The maximum energy of the ions arriving at the grounded wall is related to the plasma potential relative to ground. Typical ion energy distributions are shown in Fig. 7. The results in Fig. 7(a) are for the same discharge conditions as in Fig. 6(a). The maximum ion energy is about 75 eV for an applied field of 200 G and about 80 eV at zero magnetic field. When the ion transit time through the sheath is much less than the rf period, the maximum ion energy will be equal to the maximum excursion of the plasma potential above ground and the time dependence of floating potential will have the form typical of resistive sheaths. The temporal variation in floating potential for the 200-G case in Fig. 3 is suggestive of largely resistive sheaths. Therefore, it can be expected that the maximum ion energy incident on the grounded wall should be close to the maximum excursion of the plasma potential for the 200-G case. However, for the case without a magnetic field, the temporal variation in floating potential did not indicate that the sheaths were resistive. Therefore, the maximum ion energy incident on the grounded wall was expected to be less than the maximum excursion of the plasma potential. Thus we estimate that the radial variation in plasma potential across the discharge plasma for the 200-G case shown in Fig. 6(a) has the form shown schematically in Fig. 8(a).

The measured ion energy distributions at 13.56 MHz with magnetic field strengths of zero and 200 G are shown in Fig. 7(b). The data in Fig. 4 show that the variation in floating potential at 13.56 MHz exhibits the sinusoidal behavior one would expect for a discharge with primarily capacitive sheaths. Where the transit time of the ions through the sheath is longer than the rf period and there is no dc bias, the maximum in the ion energy distribution will be at V_0/π, where V_0 is the maximum value of the plasma potential relative to ground.[15] To the extent that this relationship can be used as an approximation for cases with a dc bias, we note that the peaks in the distributions in Fig. 7(b) occur at about 20 eV for the zero magnetic field case and about 28 eV for the 200-G case. This would imply the maximum plasma potentials relative to ground are about 65 and 90 eV, respectively,

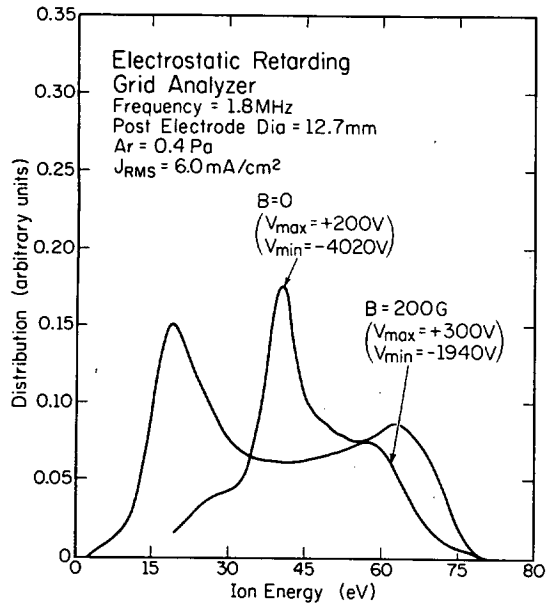

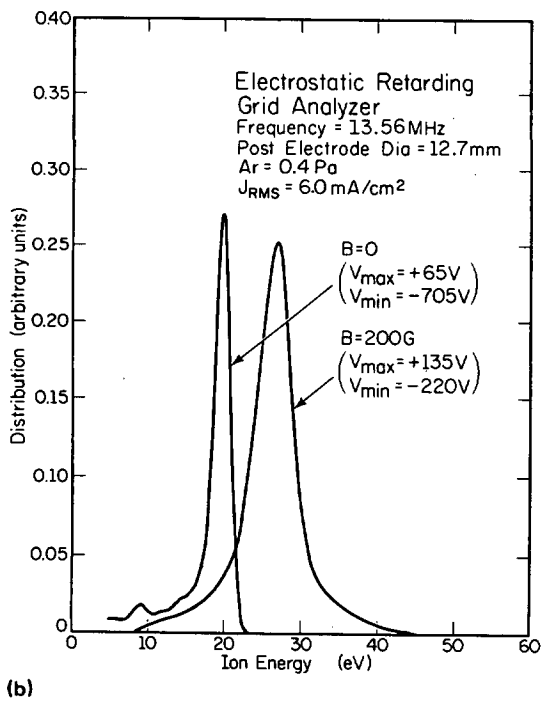

FIG. 7. Energy distribution of ions incident on the chamber wall as measured with the electrostatic analyzer for a discharge using a 12.7-mm-diam post electrode driven at (a) 1.8 and (b) 13.56 MHz.

for the conditions shown in Fig. 6(b). The maximum plasma potential estimated by the energy analyzer was close to the maximum positive voltage of the post electrode for zero magnetic field case, but it was smaller than the maximum positive voltage of the electrode for the 200-G case. In both cases this would place the plasma potential about 50 to 70 eV above the floating potential, which is reasonably consistent with the offset suggested by the floating potential calculated with the average electron temperature obtained by the probe data. Thus we estimate that the radial variation in plasma potential across the discharge plasma for the 200-G case of

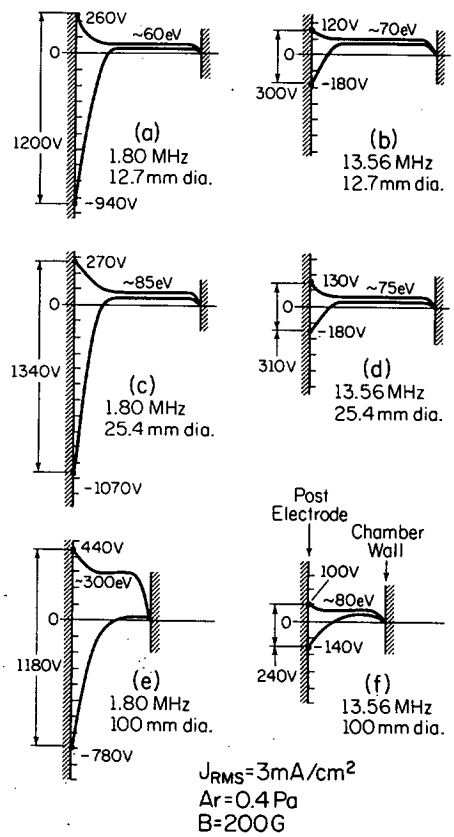

FIG. 8. Schematic summary of plasma potential vs radial position for various discharges using post electrodes driven at 1.8 and 13.56 MHz.

Fig. 6(b) has the form shown schematically in Fig. 8(b). Figures 8(c)–8(f) summarize similar plasma potential estimates for the 25- and 100-mm-diam electrodes at 3 mA/cm² with 200 G.

IV. DISCUSSION

The inverse area ratios (reciprocal of electrode area relative to chamber wall area) for the cylindrical post electrodes investigated in this paper range from about 2.5 to 18. Thus in the absence of a magnetic field we should expect dc self-bias voltages in the range from 80% to 95% of the zero-to-peak applied voltage.[7] The experimental observations at zero magnetic field are consistent with this expectation (Fig. 2). However, when the magnetic field was increased to 200 G the dc self-bias was reduced to between 20% and 60% of the zero-to-peak voltage. We believe that this behavior is a consequence of the effect of the magnetic field in reducing the electron mobility in directions perpendicular to the axis of the central post electrode.

Glow-discharge magnetrons of the type generally used for sputtering and discussed in this paper are usually designed according to a dc concept. This design criteria requires specific configurations and orientations of the cathode, anode, and magnetic field which act in concert to form an azimuthally symmetric electron trap, or traps, over the cathode surface.[9,10] The primary electrons, which leave the cathode surface via secondary emission due to ion bombard-

ment are accelerated in the cathode dark space and exchange energy through collisional and plasma oscillation processes as they migrate across the magnetic field to reach the anode. The anode is ideally positioned to intersect magnetic field lines at the periphery of the trap. This energy exchange provides efficient ionization and permits intense discharges to be sustained, even at low pressures.

The dc magnetron concept is designed to improve the effectiveness of the ionization process in cold cathode discharges which are sustained primarily by the ionizing action of secondary electrons released from the cathode surface by energetic ion bombardment. Magnetron configurations may also improve the ionizing efficiency of rf discharges which operate at modest frequencies and where secondary electrons play a significant role in the overall ionization process.[18-20] The spatial dependence of plasma potential for the various discharges driven at 1.8 MHz [summarized in Figs. 8(a), 8(c), and 8(e)] shows that the negative electrode voltage swings are in the range from 700 to 1100 V. The magnitude of these voltages and the radial dependence of the plasma potentials suggest that the discharge is largely sustained by secondary electron emission during the negative half cycle. Therefore, the discharges resemble dc cylindrical magnetron discharges. Measurements of ion saturation currents indicate that the electron densities, for the 1.8-MHz case of Fig. 8, were in the range 2×10^{10}–10^{11} cm^{-3} near the powered electrode within the end flange.[13] These values are typical of those seen for dc magnetrons operated under similar current densities and provide further support for the proposition that the discharge that forms during the negative rf voltage cycle resembles a post magnetron. However, when the voltage of the center electrode swings positive, relatively large voltage drops develop adjacent to the anode as shown in Figs. 8(a), 8(c), and 8(e) (100–200 V). Time-dependent electrostatic probe and light emission measurement also indicate that a reversed polarity hollow cathode discharge does not form with smaller post electrodes [Figs. 8(a) and 8(c)] as shown by the large voltage drop developed near the anode.[13]

At high frequencies glow discharges tend to be sustained by energetic electrons that are heated within the plasma volume by the oscillating electric fields.[15] In the 13.56-MHz cases shown in Figs. 8(b), 8(d), and 8(f), the discharges appear to be operating in the volume electron heating regime. The sheaths exhibit capacitive behavior. The rms voltages are typically a factor of 4 less than in the 1.8-MHz cases. Although the magnetron concept is not specifically designed to assist the ionization process in this type of discharge, the magnetic fields can be expected to reduce wall losses and promote volume electron heating and ionization in desirable regions adjacent to the electrodes. This proposition is supported by the observation that the discharges which formed in the magnetron electrode systems at 13.56 MHz had electron densities (2×10^{10}–10^{11} cm^{-3}) near the powered electrode that were typical of dc magnetrons driven at comparable power levels and more than an order of magnitude higher than those found in the absence of magnetic fields [$(1-3\times)10^{9}$ cm^{-3}].[13] Time-dependent electrostatic probe and light emission measurements indicated an increase in electron density during the negative part of the rf cycle and a slight decay (20%–30%) during the positive voltage swing, indicating that little additional ionization occurred during the positive "anode" cycle. The positive voltage swings are also considerably less than in the 1.8-MHz case. However, these resulting self-bias levels are relatively small, typically values being about 20% at 200 G as shown in Fig. 2.

The maximum plasma potentials associated with the 13.56-MHz discharges were close to the maximum voltage of the post electrode but there was a certain voltage drop (20–60 V) that developed adjacent to the post electrode. This voltage is apparently required to draw an electron current that is equal to the ion flux during the remainder of the rf cycle and therefore to satisfy the current conservation requirement for rf capacitive discharges. This voltage drop is believed to be a consequence of the axial magnetic field, which reduces the electron mobility in the radial direction as described in detail in Ref. 13. For a 200-G field perpendicular to the electric field, the radial electron current transport can be expected to be reduced significantly.[20]

Therefore, as the axial magnetic field strength is increased, the dc self-bias voltage must decrease as shown in Fig. 2. This results from the reduction in the electron mobility in directions perpendicular to the axis of the post electrode when it serves as anode and because of the increase in electron trapping near the post electrode and reduction in the electron losses to the wall when it serves as cathode.

The time-dependent electrostatic double probe data showed that for 12.7- and 25.4-mm-diam electrodes at 1.8 MHz, the ion saturation current underwent a decay to essentially zero. For the 100-mm-diam electrode at 1.8 MHz, the ion saturation current showed a modulation of about 65%, while at 1.8 MHz the modulation was in the range of 10%–25% for all three electrodes.[13] The high percent of self-bias voltage at 1.8 MHz shown in Fig. 2 appears to result from the large decay of ion density during the anode cycle. Therefore, a large negative voltage is needed to sustain the discharge current compared to the 13.56-MHz cases, where high ion densities exist during the anode cycle.

As a check on our conclusion regarding the nature of the ion bombardment at the post electrode, a series of experiments were conducted during which the sputtering rates of stainless steel from the 25.4-mm-diam post electrode under rf power were measured. These values were compared to the dc sputtering rate at identical average currents for 1.4 Pa Ar. Large sputtering rates correlate with high rates of ion bombardment. The measurements consisted of collecting a portion of the sputtered flux on an aluminum foil located on the cathode midplane at a radius of 40 mm and weighing it. The measurements were made at rms currents of 0.5 and 1.0 A and magnetic fields of 100 and 200 G. The results are summarized in Table I. The data are presented as a thickness deposition rate, based on the assumption of a bulk density for the stainless-steel coatings.

The rf sputtering rates are consistently about 40% of the corresponding dc values in the 1.8-MHz case, and vary from near zero to about 2% of the dc values in the 13.56-MHz case. The reduced sputtering rates at 1.8 MHz are believed to

TABLE I. Relative deposition rates (Å/min) due to cathode sputtering. Post electrode diameter = 25.4 mm. Ar pressure = 0.4 Pa. Substrates at a radius of 40 mm.

Discharge current		100 G			200 G		
		dc	1.8 MHz	13.56 MHz	dc	1.8 MHz	13.56 MHz
0.5 A							
	Deposition rate (Å/min)	515	221	8.7	570	178	2.2
	Discharge voltage rf (zero-to-peak)	712 V	890 V	105 V	599 V	580 V	123 V
	Self-bias voltage (% zero-to-peak)	...	− 670 V (75%)	− 25 V (23%)	...	− 320 V (55%)	− 14 V (11%)
	Deposition rate (relative to (dc)	...	0.43	0.017	...	0.31	0.004
1.0 A							
	Deposition rate (Å/min)	1040	419	15.4	949	437	26
	Discharge voltage rf (zero-to-peak)	773 V	1390 V	133 V	685 V	970 V	135 V
	Self-bias voltage (% of zero-to-peak)	...	− 1110 V (80%)	− 45 V (34%)	...	− 650 V (67%)	− 28 V (17%)
	Deposition rate (relative to dc)	...	0.40	0.015	...	0.46	0.027

be due to two factors: (1) ion bombardment occurs only during the negative voltage swing of the post electrode, and (2) the discharge current is somewhat out of phase with the discharge voltage. As the magnetic field decreases, the dc self-bias increases, thereby increasing the fraction of the rf cycle during which energetic ion bombardment occurs. However, this increase is largely compensated by the increase in the phase difference between the current and voltage that occurs as the magnetic field is decreased as shown in Fig. 5. The lower sputtering rates at 13.56 MHz are believed to be due to the low discharge voltage, the small dc self-bias, and the fact that the ions require many cycles to cross the sheath and do not obtain the peak voltage. Consequently, the bombarding energies are near the threshold for sputtering, with the result that the sputtering rates are negligible or very small.

The expected reductions in the sputtered fluxes for the 1.8-MHz case were calculated on the assumption that the bombarding ion energies reflect the instantaneous discharge voltage $V(\theta)$ at a given point θ in the rf phase. The ratio of rf-to-dc sputtering is then

$$\frac{\mathrm{RF}_{\mathrm{rate}}}{\mathrm{DC}_{\mathrm{rate}}} = \left(\frac{I_{o\text{-}p}}{2\pi}\int_0^{2\pi} \cos(\theta + \phi) S[V(\theta)]\, d\theta\right) \Big/ I_{dc} S(V_{\mathrm{dc}}),$$

where I is the discharge current, ϕ is the phase difference between the current and voltage, and $S(V)$ is the voltage dependence of the sputtering yield. Predicted ratios were calculated using sputter yield data for iron from Ref. 21. The calculated values are in the range from 0.50 to 0.75 and therefore a little higher than the measured values. This difference is due, in part, to the poor assumption that the ion energy is equal to the instantaneous sheath voltage.

The expected reductions in the sputtered fluxes for the 13.56-MHz case were calculated on the assumption that the ions required many rf cycles to cross the sheath, so that their bombarding energy is equal to the negative sheath voltage averaged over the rf cycle, using the relationship

$$\frac{\mathrm{RF}_{\mathrm{rate}}}{\mathrm{DC}_{\mathrm{rate}}} = \frac{I_{\mathrm{rms}} S(V_{\mathrm{ave}})}{I_{\mathrm{dc}} S(V_{\mathrm{dc}})},$$

where

$$V_{\mathrm{ave}} = \frac{1}{2\pi}\int_0^{2\pi} V^-(\theta)\, d\theta$$

and $V^-(\theta)$ is the negative variation in the discharge voltage. The calculated ratios were in the range from 0 to 0.05 and therefore in reasonable agreement with the data given in Table I.

V. CONCLUSION

The formation of dc self-bias voltages in rf cylindrical-post magnetron discharge was investigated for various post diameters driven at rf frequencies of 1.8 and 13.56 MHz, and using magnetic field strengths from 0 to 200 G. The dc self-bias voltage was less for discharges using the larger diameter post electrode at fixed magnetic field strengths, as suggested by other authors for capacitively coupled parallel plate discharges,[4–6] but the dc self-bias voltage was also a strong function of magnetic field strength.

The reductions of the dc self-bias voltage in rf cylindrical magnetrons at increased magnetic fields are due to the effect on electron mobility of the magnetic field perpendicular to the electric field. When an rf capacitively coupled post electrode discharge was operated at a given current density, the positive peak voltage of the post electrode increased with increasing magnetic field and the negative peak voltage decreased. The increase in the positive peak voltage is attributed to the reduction of electron mobility

toward the post electrode when the post electrode serves as an anode. The decrease in the negative peak voltage at increased magnetic field is due to "improvement" of the electron trap near the post electrode which causes enhanced ionization when the post electrode serves as a cathode.

The reduction of electron mobility at high magnetic fields also caused a rather large voltage drop for the 1.8-MHz cases (25%–70% of the anode peak potential) and for 13.56-MHz cases (20%–40%) near the post electrode at the peak of the anode cycle. This voltage drop appears to prevent operation of a hollow-cathode-like discharge during the anode cycle for the small electrodes at 1.8 MHz. The high-voltage drop likely results from the reduction in electron mobility by the magnetic field which reduces the "return current" density of the electrons to the anode. Since the current density at the central anode must be proportionally larger to account for the difference in areas, a positive sheath voltage develops to drive the electron current. As the diameter of the central post electrode increases, the disparity in current densities decreases, and the anode sheath potential also decreases. Time-averaged conductivity was increased as the magnetic field was increased because the amount of increase in the conductivity during the negative half cycle was larger than that of the decrease in conductivity during the positive half cycle. Generally, the conductivity for 13.56-MHz cases was higher than that for 1.8-MHz cases as a consequence of the increased volume ionization for 13.56-MHz cases compared to that for 1.8 MHz cases. It was demonstrated by the temporal ion density measurement that the ion densities at 1.8 MHz decayed more than the 13.56-MHz cases during the anode cycle. The high dc self-bias voltage at 1.8 MHz compared to 13.56 MHz cases could be explained by the large decay of ion densities for 1.8-MHz cases during the anode cycle.

ACKNOWLEDGMENTS

Professor John A. Thornton died unexpectedly in November 1987. He contributed significantly to this work and his guidance will be missed. The authors wish to express their gratitude to Dr. Alan Penfold for his helpful discussions and suggestions. This work was supported by the Joint Services Electronics Projects Agency under Contract No. N00014-84-C-0149.

[1] B. Chapman, *Glow Discharges Processes* (Wiley, New York, 1980).
[2] G. K. Wehner and G. S. Anderson, in *Handbook of Thin Film Technology*, edited by L. I. Maissel and R. Glang (McGraw-Hill, New York, 1970), pp. 3-1 to 3-38.
[3] H. S. Butler and G. S. Kino, Phys. Fluids **6**, 1346 (1963).
[4] H. R. Koenig and L. I. Maissel, IBM J. Res. Dev. **14**, 168 (1970).
[5] J. W. Coburn and E. Kay, J. Appl. Phys. **43**, 4965 (1972).
[6] C. M. Horwitz, J. Vac. Sci. Technol. A **1**, 60 (1983).
[7] S. E. Savas, in *Plasma Processing and Synthesis of Materials*, edited by D. Apelin and J. Szekely (Materials Research Society, Pittsburgh, PA, 1987), p. 35.
[8] J. H. Keller and W. B. Pennebaker, IBM J. Res. Dev. **23**, 3 (1979).
[9] J. A. Thornton and A. S. Penfold, in *Thin Film Processes*, edited by J. L. Vossen and W. Kern (Academic, New York, 1978), p. 75.
[10] J. A. Thornton, Thin Solid Films **80**, 1 (1981).
[11] J. A. Thornton (unpublished data).
[12] I. Lin, J. Appl. Phys. **58**, 2981 (1985).
[13] G. Y. Yeom, J. A. Thornton, and M. J. Kushner, J. Appl. Phys. **65**, 3816 (1989).
[14] G. Y. Yeom, J. A. Thornton, and A. S. Penfold (unpublished).
[15] R. H. Bruce, J. Appl. Phys. **52**, 7064 (1981).
[16] K. Köhler, J. W. Coburn, D. E. Horne, E. Kay, and J. H. Keller, J. Appl. Phys. **57**, 59 (1985).
[17] K. Köhler, D. E. Horne, and J. W. Coburn, J. Appl. Phys. **58**, 3350 (1985).
[18] M. J. Kushner, J. Appl. Phys. **54**, 4958 (1983).
[19] M. J. Kushner, IEEE Trans. Plasma Sci. **PS-14**, 188 (1986).
[20] J. A. Thornton, J. Vac. Sci. Technol. **15**, 171 (1978).
[21] N. Laegreid and G. K. Wehner, *Sixth National Symposium on Vacuum Technology Transactions* (Pergamon, New York, 1960), p. 164.